Heat Mass Transfer (2012) 48:1089–1101
DOI 10.1007/s00231-011-0957-7

ORIGINAL

Analysis of exergy and parametric study of a v-corrugated solar air heater

Mahdi Hedayatizadeh · Yahya Ajabshirchi · Faramarz Sarhaddi · Said Farahat · Ali Safavinejad · Hossein Chaji

Received: 7 October 2010 / Accepted: 22 December 2011 / Published online: 5 January 2012

Abstract Solar air heater requires investigation for enhancement of solar energy conversion into heat. Different configurations with various artificial roughness geometries are proposed to date. In present study attention is paid on ways leading to more delivery of exergy by a v-corrugated solar air heater through parametric study. Effects of aspect ratio of the collector, inlet air temperature, mass flow rate per collector area etc. are studied.

List of symbols

L	Length of collector (m)
W	Width of collector (m)
A	Collector area ($L \times W$) (m^2)
Q_u	Useful heat energy gain of the collector (W)
$\dot{m}$	Mass flow rate of air through collector (kg/s)
$\dot{M}$	$\dot{m}$ Divided by collector area (kg/m^2 s)
G	Mass flux in passage, $\dot{m}$ divided by passage area (kg/m^2 s)
T	Temperature (K)
C_p	Specific heat (J/kg K)
U_b	Bottom heat loss coefficient (W/m^2 K)
U_t	Top heat loss coefficient (W/m^2 K)
U_L	Total heat loss coefficient (W/m^2 K)
V	Velocity (m/s)
W_p	Pump work (W)
S	Absorbed flux of sun radiation (W/m^2)
S_g	Entropy created due to heating of air and pressure drop (W/K)
Re	Reynolds number
D_h	Hydraulic diameter of the passage (m)
b	One-half altitude of the v-corrugated passage (m)
F_R	Collector heat removal factor
F'	Collector efficiency factor
IR	Irreversibility (W)
$I_{T,c}$	Radiation incident on glass cover (W/m^2)
h	Convective heat-transfer coefficient (W/m^2 K)
p	Pressure (N/m^2)
h_1	Convective heat transfer coefficient between flowing air and the absorber (W/m^2 K)
h_2	Convective heat transfer coefficient between flowing air and the bottom surface (W/m^2 K)
Ex	Exergy (W)
$Ex_{u,p}$	Exergy output rate including pressure drop (W)
n	Number of collectors connected in series
k	Thermal conductivity (W/m K)
F	Friction factor
N	Number of glass covers
Nu	Nusselt number
Δp	Difference in pressure (Pa)

M. Hedayatizadeh (✉) · Y. Ajabshirchi · H. Chaji
Department of Agricultural Machinery Engineering,
Faculty of Agriculture, University of Tabriz, Tabriz, Iran
e-mail: mhedayatizadeh@gmail.com

M. Hedayatizadeh
Faculty of Agriculture, University of Birjand,
P.O. Box 97175/331, Birjand, Iran

F. Sarhaddi · S. Farahat
Department of Mechanical Engineering, Faculty of Engineering,
University of Sistan and Baluchestan, P.O. Box 98164/161,
Zahedan, Iran

A. Safavinejad
Department of Mechanical Engineering, Faculty of Engineering,
University of Birjand, Birjand, Iran

H. Chaji
Ministry of Agriculture, Center of Agriculture and Natural
Resources of Khorasan Razavi Province, Mashhad, Iran

Greek symbols

ψ	Exergy efficiency of radiation
α	Absorptivity
τ	Transmitivity
φ	Tilt angle of the collector
η	Efficiency
Δ	Thickness (m)
ρ	Density of fluid (kg/m^3)
μ	Viscosity (N s/m^2)
ε	Emissivity
σ	Stefan's constant

Subscripts

a	Ambient
b	Bottom
c	Collector
en	Energy
ex	Exergy
f	Fluid
g	Glass
i	Insulation/inlet
m	Mean
o	Outlet
p	Plate
pm	Pump-motor/mean-plate
r	Radiation
S	Sun
t	Top
w	Work/wind

1 Introduction

Solar air heaters (SAHs) are kinds of heat exchangers that transform solar energy into heat. They are usually used for heating air in drying agricultural products and as an air heater in combination with auxiliary heaters for air conditioning of buildings [1]. The conventional method of drying of agricultural products in developing countries is the open-air sun drying method while the post-harvest losses of agricultural products can be reduced by using a well-designed solar drying system. Since the air collector is the most important component of a solar food drying system, an improvement in the design of collectors would lead to a better performance of the system. Application of solar energy systems, such as solar drying, requires collectors of high efficiency [2]. But the efficiency of SAHs has been found to be low because of the low convective heat transfer coefficient between absorber plate and the flowing air which increases the absorber plate temperature. To overcome this problem, different remedies were applied. For instance, the double-flow type SAHs were introduced for increasing the heat-transfer area, leading to improved thermal performance. This increases the thermal energy transfer between the absorber plate and the air, which clearly improves the thermal performances of the solar collectors. Moreover, obstacles arranged into the air channel duct seem promising. These obstacles allow a good distribution of the fluid flow [3]. Akpinar and Koçyiğit [4] investigated experimentally the performance analysis of a flat-plate solar air heater having special obstacles and compared with the one without obstacle. They got that the highest efficiency was obtained by the SAH with the leaf shaped obstacles on the absorbent plate in flow channel duct for all operating conditions, whereas the lowest values was obtained for the SAH without obstacles. They concluded that the efficiency of the solar air collectors depends significantly on the solar radiation, surface geometry of the collectors and extension of the air flow line. Alta et al. [5] did an experimental investigation of three different flat-plate SAHs (two having fins and one without fin) with different number of glass covers, air flow rates and tilt angles to find their effects on the energy and exergy. Based on the energy and exergy output rates, heater with double glass covers and fins is more effective and the difference between the input and output air temperature is higher than that of the others. Moreover, the authors concluded that the circulation time of air inside the heater played a role more important than the number of transparent sheets and in the applications of which temperature differences is more important, lower air flow rates should be preferred. Tyagi et al. [6] presented a comparative experimental study based on energy and exergy analyses of a typical solar air heater collector with and without temporary heat energy storage (THES) material, viz. paraffin wax and hytherm oil. Based on the experiments performed, they calculated the energy and exergy efficiencies with respect to the available solar radiation for three different arrangements, viz. one arrangement without heat storage material and two arrangements with THES, viz. hytherm oil and paraffin wax, respectively. It is found that both the efficiencies in case of heat storage material/fluid are significantly higher than that of without THES, besides both the efficiencies in case of paraffin wax are slightly higher than that of hytherm oil case. Corrugated collectors with different profiles, also, increasing the area of the air-surface contact was another way for enhancement of the solar collector performance. On the other hand, the major problem associated with solar collectors is to collect and deliver solar energy to users with minimum losses [7]. But, it should be taken into consideration that the energy equation alone does not include the internal losses; in other words, it cannot be a sufficient criterion for the solar collector efficiency. Hence, the second law of thermodynamics seems influential for quantifying the inefficiencies, their relative magnitudes and where they occur [8]. Hence, Exergy analysis, derived from both the first and second laws of thermodynamics, as compared to energy analysis, takes into account the quality of the energy transferred. Exergy (or availability) analysis is a powerful tool in the design, optimization, and performance evaluation of energy systems. This analysis can be used to identify the main sources of irreversibility (exergy loss) and to minimize the generation of entropy in a given process where the transfer of energy and material take place [9]. There are not so many studies concentrated on the exergy analysis of solar air collectors which necessitates more required work [10–12]. The energy efficiency, friction factor and dimensionless exergy loss of a solar air heater having five solar sub-collectors of the same length and width arranged in series in a common case, for various values of Reynolds number were investigated by Kurtbas and Durmus [13]. It is important to mention that the popularity of exergy analysis method has grown consequently and is still growing [14]. A review on exergetic analysis and estimation of renewable energy resources for sustainable future for solar collector, solar drying, solar desalination, solar thermal power plants, and hybrid PV thermal solar collector was performed by Hepbasli [15]. Suzuki [16] discussed about the various terms like exergy inflows, exergy leakage and exergy annihilation (destruction) related to the general theory of exergy balance, and applied these to flat plate and evacuated solar collectors. He evaluated the effect of heat capacity on various exergy loss terms and exergy gain by the working fluid. Lin et al. [17] carried out a comprehensive parametric study on thermal performance of cross-corrugated solar air collectors to find the effects of different parameters on the collector performance. They selected three types of solar collectors and perceived that the collector with a wavelike absorbing plate and a wavelike bottom plate is highly superior to the one with both the channel plates being smooth. They also concluded that to achieve a higher collector efficiency, it is essential to construct the collectors having slender configurations along the air flow direction, to maintain a small mean gap between the absorbing plate and bottom plate, to maintain a higher air mass flow rate, and to operate the collectors with the inlet fluid temperature close to that of the ambient fluid. Qi et al. [18] applied the Taguchi method as a well-known parametric study tool in engineering quality and experimental design. They performed analysis on five experimental factors (flow depth, ratio of fin pitch and fin thickness, tube pitch, number of louvers and angle of louver) affecting the heat transfer and pressure drop of a heat exchanger with corrugated louvered fins. Their results confirmed that flow depth, ratio of fin pitch and fin thickness and the number of the louvers are the main factors that influence significantly the thermal hydraulic performance of the heat exchanger with corrugated louvered fins. Also a detailed theoretical parametric analysis of a corrugated solar air heater with and without cover was performed by Verma et al. [19]. They investigated the optimum flow channel depth, at which the maximum heat is available at the lowest collector cost. They also, observed the effect of collector parameters and operating conditions on the collector performance. The triangular duct flow channel with v-corrugated absorber has a significant advantage in absorbing a greater quantity of solar radiation and some increased heat transfer to the transport fluid as compared to the plane surface absorber with rectangular duct [20]. To our knowledge, a few investigations are performed on the exergetic and parametric study of v-corrugated SAH together yet, though, Liu et al. [21] performed a parametric study on the thermal performance of a solar air collector with a v-corrugated absorber. The objective of the present work is to analyze the v-corrugated solar air heater from the exergetic point of view and also to investigate the design parameters affecting its performance.

2 Theoretical analysis

2.1 Analysis of solar absorber

Many researchers have worked on analytical investigation of the SAH, such as Hottel and Woertz [2]. In Fig. 1, the schematic front view of the v-corrugated solar air heater is shown. The collector considered includes a flat glass cover to decrease heat losses from the top of the heater and a v-corrugated absorber plate having a well insulated bottom plate which forms a passage through which the air to be heated flows. Air flowing through each triangular-shaped corrugation removes heat from the absorber and such a heat energy produced can be used for different applications.

The following equations dealing with the steady state efficiency of the solar air collector, may give rise to calculation of heat gain by air:

$$Q_u = \dot{m}C_p(T_o - T_i) \tag{1}$$

$$Q_u = A_c\left[S - U_L\left(T_{pm} - T_a\right)\right] \tag{2}$$

$$\begin{aligned} Q_u &= A_cF_R[S - U_L(T_i - T_a)] \\ &= A_cF_R\left[\tau_g\alpha_pI_{T,c} - U_L(T_i - T_a)\right] \end{aligned} \tag{3}$$

where Q_u, $\dot{m}$, C_p, T_o, T_i, T_{pm}, T_a, A_c, $I_{T,c}$, S, U_L, F_R, τ_g and α_p are the useful heat gain, mass flow rate, specific heat capacity, outlet air temperature, inlet air temperature, mean plate temperature, ambient temperature, collector area, radiation incident on glass cover, absorbed solar radiation, total heat loss coefficient, collector heat removal factor, transmitivity of glass cover and absorptivity of absorber plate, respectively.

The collector heat removal factor is defined as follows [22]:

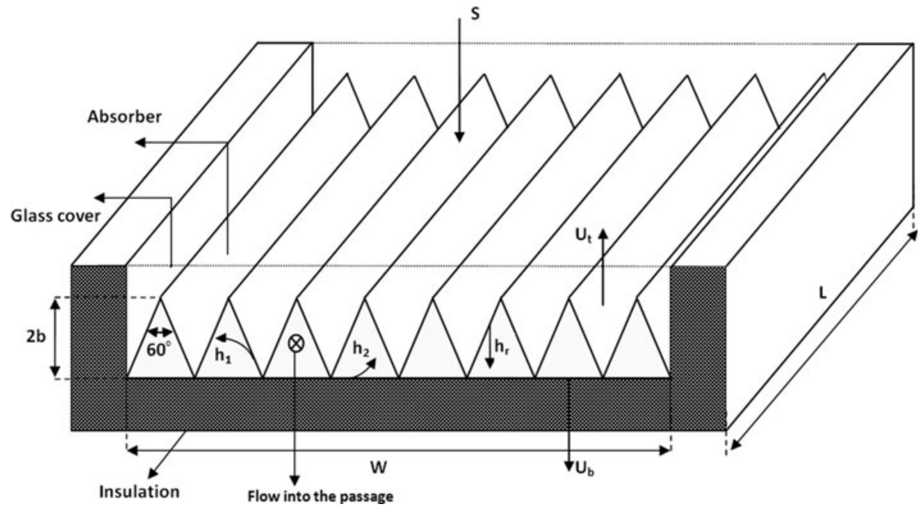

Fig. 1 Front view of the v-corrugated solar air heater

$$F_R = \frac{\dot{m}C_p}{U_L A_c}\left[1 - \exp\left(\frac{-U_L A_c F'}{\dot{m}C_p}\right)\right] \tag{4}$$

In which the collector efficiency factor F' is given by

$$F' = \frac{2h_1(h_2 + h_r) + h_r h_2}{(h_r + h_2)(2h_1 + U_L) + h_r h_2} \tag{5}$$

where h_1, h_2 and h_r are the convective heat transfer coefficient between flowing air through the passage and the absorber, convective heat transfer coefficient between flowing air and the bottom surface and radiative heat transfer coefficient between the absorber and the bottom surface, respectively.

The total heat loss coefficient U_L of the collector is given by

$$U_L = U_b + U_t$$

in which U_t and U_b are the top and bottom heat loss coefficients, respectively.

To calculate U_t, an empirical equation given by Klein, is applied [22]:

$$U_t = \left[\frac{N}{\left(\frac{C}{T_{pm}}\right)\left[\frac{T_{pm}-T_a}{N+f}\right]^e} + \frac{1}{h_w}\right]^{-1} + \frac{\sigma(T_{pm}+T_a)(T_{pm}^2+T_a^2)}{\left[\varepsilon_p + 0.00591Nh_w\right]^{-1} + \left[\frac{(2N+f-1+0.133\varepsilon_p)}{\varepsilon_g}\right] - N} \tag{6}$$

where $f = (1 + 0.089h_w - 0.1166h_w\varepsilon_p)(1 + 0.07866N)$, $C = 520(1 - 0.000051\varphi^2)$ for $0^\circ < \varphi < 70^\circ$. Use $\varphi = 70^\circ$ when $70^\circ < \varphi < 90^\circ$.

$$e = 0.43\left(1 - \frac{100}{T_{pm}}\right)$$

where N, h_w, ε_p, ε_g, σ and φ are the number of glass covers, convection heat transfer coefficient from the glass cover due to wind, emissivity of plate, emissivity of glass, Stefan's constant and collector tilt, respectively. It must be mentioned that U_t is based on the projected area [22].

The convection heat transfer coefficient from the glass cover due to wind is recommended by McAdams [23] as

$$h_w = 2.8 + 3V_w \tag{7}$$

where V_w is the speed of wind on glass cover of the collector. The bottom heat loss coefficient is also calculated from equation given as

$$U_b = \frac{k_i}{\Delta_i} \tag{8}$$

where k_i and Δ_i are the thermal conductivity of insulation and thickness of insulation at the bottom of collector.

Combining Eqs. 2 and 3 leads to finding T_{pm} given by

$$T_{pm} = T_a + \frac{1}{U_L A_c}(SA_c - Q_u) \tag{9}$$

While the fluid temperature, T_f and mean bottom plate temperature, T_{bm}, are given as follows:

$$T_f \cong \frac{T_i + T_o}{2} = \frac{Q_u}{\dot{m}C_p} + T_i \tag{10}$$

$$T_{bm} = \frac{U_b T_a + h_r T_{pm} + h_1 T_f}{U_b + h_r + h_1}. \tag{11}$$

2.2 Heat transfer and friction coefficients

The radiation heat transfer coefficient between absorber plate and insulation plate may be calculated by

$$h_r = \frac{\sigma\varepsilon_b\varepsilon_p(T_{bm}^2 + T_{pm}^2)(T_{bm} + T_{pm})}{\varepsilon_b + \varepsilon_p - \varepsilon_b\varepsilon_p} \tag{12}$$

where ε_b and ε_p are emissivity of bottom plate (insulation) and emissivity of absorber plate, respectively.

For the fluid moving between the absorbing and the bottom plates, h_1 and h_2 representing convection heat-transfer coefficients between flowing air and absorber plate and bottom plate, respectively are assumed equal. Hollands and Shewen [24] suggested that the Nusselt number, Nu, for an equilateral triangle arrangement can be expressed as:

$$Nu = Nu_0 + \beta \frac{b}{L} n \tag{13}$$

where b, L and n are one-half altitude of the v-groove, length of collector and number of collectors connected in series, respectively. Nu_0 and β are functions of Reynolds number $\left(\frac{b}{L} < 8 \times 10^{-3}\right)$. Hollands [24] recommended following relationships for different flow conditions.

For laminar flow ($Re < 2{,}800$):

$$Nu_0 = 2.821 \tag{14}$$

$$\beta = 0.126 Re \tag{15}$$

For transient flow ($2{,}800 \leq Re \leq 10^4$):

$$Nu_0 = 1.9 \times 10^{-6} Re^{1.79} \tag{16}$$

$$\beta = 225 \tag{17}$$

For early turbulent flow ($10^4 < Re < 10^5$):

$$Nu_0 = 0.0302 Re^{0.74} \tag{18}$$

$$\beta = 0.242 Re^{0.74} \tag{19}$$

Finally the convective heat transfer coefficient h can be calculated from the following equations:

$$Nu = \frac{hD_h}{k_a} \quad \text{and} \quad D_h = \frac{4b}{3} \quad \Rightarrow h = \frac{3k_a Nu}{4b} \tag{20}$$

where D_h, k_a and Re are the hydraulic diameter of the flow passage, thermal conductivity of air and Reynolds number, respectively.

The mass flow rate through the collector is $\dot{m} = \dot{M} \times L \times W$ and the mass flux through the passage is $G = \frac{\dot{m}}{(b \times W)}$ or $\frac{\dot{M} \times L}{b}$ is seen to be independent of W.

Reynolds number is calculated by

$$Re = \frac{GD_h}{\mu} = \left(\frac{\dot{M} \times L}{b}\right)\left(\frac{1}{\mu}\right)\left(\frac{4b}{3}\right) = \frac{4\dot{M}L}{3\mu} \tag{21}$$

where $\dot{M}$, W and μ are mass flow rate of air through collector divided by collector area, width of collector and viscosity of air, respectively.

When the air temperature varies in the range of 280–470 K, the following empirical correlations can be obtained from [21, 25] to estimate the density, ρ_a, thermal conductivity, k_a, and dynamic viscosity, μ_a, of air:

$$\rho_a = 3.9147 - 0.016082 T_f + 2.9013 \times 10^{-5} T_f^2 - 1.9407 \times 10^{-8} \times T_f^3 \tag{22}$$

$$k_a = \left(0.0015215 + 0.097459 T_f - 3.3322 \times 10^{-5} T_f^2\right) \times 10^{-3} \tag{23}$$

$$\mu_a = \left(1.6157 + 0.06523 T_f - 3.0297 \times 10^{-5} T_f^2\right) \times 10^{-6} \tag{24}$$

While $C_p \approx 1{,}000\,\mathrm{J/kg\ K}$ can be assumed.

When air flows through the passage, owing to friction, the air pressure drops along the length of the flow passage. The pressure drop ΔP can be computed from the relation [24]:

$$\Delta P = \frac{3}{2} \frac{\dot{M}^2}{\rho_a} \left[\frac{L}{b}\right] F \tag{25}$$

where F is the mean apparent friction factor for flow in the passage calculated as follows [24]:

$$F = F_0 + \gamma \frac{b}{L} n \tag{26}$$

For laminar flow ($Re < 2{,}800$):

$$F_0 = \frac{13.33}{Re} \tag{27}$$

$$\gamma = 0.65 \tag{28}$$

For transient flow ($2{,}800 \leq Re \leq 10^4$):

$$F_0 = 3.2 \times 10^{-4} Re^{0.34} \tag{29}$$

$$\gamma = 2.94 Re^{-0.19} \tag{30}$$

For early turbulent flow ($10^4 < Re < 10^5$):

$$F_0 = 0.0733 Re^{-0.25} \tag{31}$$

$$\gamma = 0.51. \tag{32}$$

2.3 Exergy output rate

If the solar air heater (Fig. 1) is considered as a control volume, the law of exergy balance results in:

$$Ex_i + Ex_S + Ex_W = Ex_o + IR \tag{33}$$

where Ex_i, Ex_o, Ex_S, Ex_W and IR are the exergy associated with the mass flow of air entering the control volume, exergy of mass flow of air leaving the control volume, exergy of solar radiation falling on glass cover, exergy of work input required to pump the air through the solar air heater, and the irreversibility of the air heating process. Due to the heat flux incident on the transparent cover, absorption by the absorber surface and heat loss to the ambient, exergy loss or irreversibility occurs. The useful exergy gain, $Ex_{u,p}$, including the pressure drop or blower work, by air through the flow in passage is given by

$$\begin{aligned} Ex_{u,p} &= Ex_o - Ex_i - Ex_w \\ &= \dot{m}C_p\left[(T_o - T_i) - T_a \ln\frac{T_o}{T_i}\right] - \frac{T_a}{T_i}W_p \end{aligned} \tag{34}$$

where W_p is the pump work. Combining Eqs. 3 and 34 gives the following equation which more clearly represents the effect of different factors on exergy

$$\begin{aligned} Ex_{u,p} &= A_cF_R\left[\tau_g\alpha_pI_{T,c} - U_L(T_i - T_a)\right] \\ &\quad - \dot{m}C_pT_a \ln\left(1 + \frac{A_cF_R}{T_i\dot{m}C_p}\left[\tau_g\alpha_pI_{T,c} - U_L(T_i - T_a)\right]\right) \\ &\quad - \frac{T_a}{T_i}W_p \end{aligned} \tag{35}$$

While the sum of entropy created term is defined by

$$S_g = \dot{m}C_p \ln\left(\frac{T_o}{T_i}\right) + \left(\frac{W_p}{T_i}\right) \tag{36}$$

The pump (blower) work W_p is calculated as follows:

$$W_p = \frac{\dot{m}\Delta P}{\eta_{pm}\rho_a} \tag{37}$$

and η_{pm} is considered as the efficiency of the pump-motor equal to 0.85 [26].

The energy efficiency of solar air heater based on first law of thermodynamics is calculated by

$$\eta_{en} = \frac{Q_u}{I_{T,c}A_c} \tag{38}$$

While the exergy collection efficiency based on second law of thermodynamics, by taking exergy of sun radiation, can be written as [14]

$$\eta_{ex} = \frac{Ex_{u,p}}{A_cI_{T,c}\psi_S} = \frac{Ex_{u,p}}{A_cI_{T,c}\left(1 - \frac{4}{3}\left(\frac{T_a}{T_S}\right)\right) + \frac{1}{3}\left(\left(\frac{T_a}{T_S}\right)^4\right)} \tag{39}$$

where T_S and ψ_S are the Sun temperature and exergy efficiency of radiation, respectively. Sun temperature is evaluated by the simple relation as follows [27]:

$$T_S = 0.055T_a^{1.5}. \tag{40}$$

3 Numerical solutions

Observing Eq. 34, $Ex_{u,p}$ is the function of different parameters such as mass flow rate, inlet/outlet and ambient air temperatures etc. The objective is to investigate the optimum mass flow rate considering given inlet and ambient temperatures of air bringing about the maximum exergy gained by the air flow. To have a numerical appreciation of the results, parameters of a v-corrugated air collector brought in Table 1 are considered and codes have been developed in MATLAB.

Table 1 Values of parameters used in MATLAB code

Parameter	Value
A_c	2 m^2
k_i	0.079 W/m K
Δ_i	5 cm
α_p	0.96
ε_p	0.95
ε_g	0.88
ε_b	0.95
τ_g	0.88
φ	30°
T_i	30–60°C
T_a	30°C
V_w	2.5 m/s
$\dot{M}$	0–350 kg/m^2 h
$I_{T,c}$	700–1,000 W/m^2
b	1–5 cm
C_p	1,000 J/kg K

To investigate the exergy and energy output rates of the v-corrugated absorber, initial guesses are made for T_{pm}, T_f and T_{bm}. Then, the heat-transfer coefficients are calculated using Eqs. 12–21. Having the new values of mean absorber, bottom plate and fluid temperatures with Eqs. 3–8 give rise to the values of useful heat gain. Afterwards, the new values of T_{pm}, T_f and T_{bm} are calculated using Eqs. 9–11. Being a difference between new values of T_{pm}, T_f and T_{bm} with their corresponding previously assumed values leads to the next iteration with the new values until the absolute difference of the new and the previous values of mean absorber plate, fluid and mean bottom plate temperatures are $\leq$0.01°C. In each step, air properties (ρ_a, k_a and μ_a) are found at T_f using Eqs. 22–24. Finally, calculated values of T_{pm}, T_{bm} and T_f are used to estimate the exergy and energy output rate using Eqs. 38 and 39.

4 Results and discussion

4.1 Variations of heat energy gain and entropy created term ($T_a \times S_g$) with mass flow rate and inlet air temperature

Variations of two important factors of heat energy gain and entropy created term ($T_a \times S_g$) with mass flow rate and for two status of low and high inlet temperatures of air are brought in Figs. 2 and 3, respectively while values of altitude of each triangular duct (2b), solar radiation (I), collector aspect ratio (AR) defined as the ratio of length to width of the collector and ambient temperature (300 K) are considered fixed. As seen, for low and high inlet temperatures of air, heat gain and entropy created terms follow an increasing trend with mass flow rate while in the latter case, the numerical values of both are lower compared with the first case. For instance, the value of heat energy gain at mass flow rate of 100 kg/(m^{2}h) is 1,131 and 785.7 W for $T_i =$ 300 and 330 K, respectively; Hence, making a decision based on only heat energy gain recommends lower inlet temperatures of air for better performance of SAH while the difference between heat energy gain and entropy created term namely exergy does not follow the same trend.

On the other hand, exergy is a more important factor which enables us to make a more rational decision about

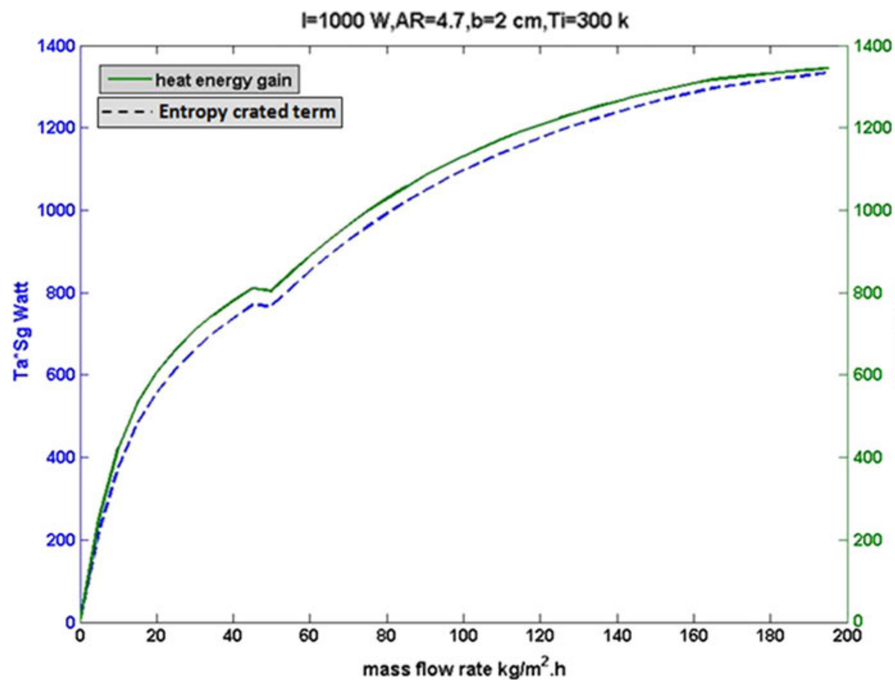

Fig. 2 Variation of useful heat gain and entropy crated term ($T_a \times S_g$) for a fixed value of solar radiation intensity and low inlet temperature of air

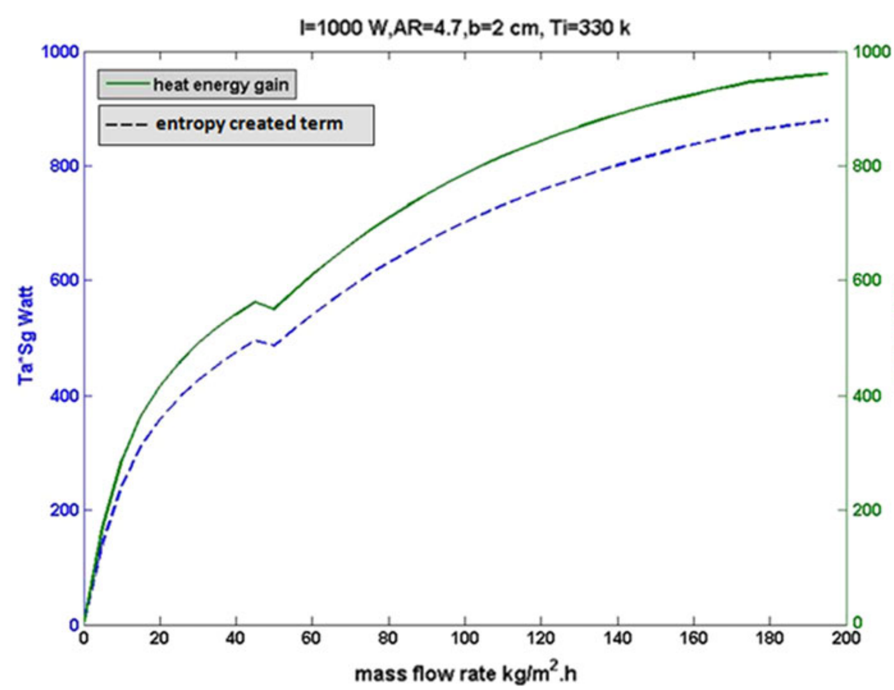

Fig. 3 Variation of useful heat gain and entropy crated term ($T_a \times S_g$) for a fixed value of solar radiation intensity and high inlet temperature of air

the modifications which seem necessary to the heater. As the result, the trend of exergy should be carefully considered which is discussed in the next part.

In both figures, a kind of a step is obvious which is more attributed to the transition of flow regime from laminar to the turbulent mode and consequently change of correlations of heat transfer coefficients and friction factor.

4.2 Variations of heat energy gain and exergy output rate with mass flow rate and inlet air temperature

In this section, variations of exergy with mass flow rate for the same values of solar radiation, collector AR and duct altitude with low and high inlet air temperatures are discussed and shown in Figs. 4 and 5, respectively. As seen, the exergy output rate increases sharply with mass flow rate

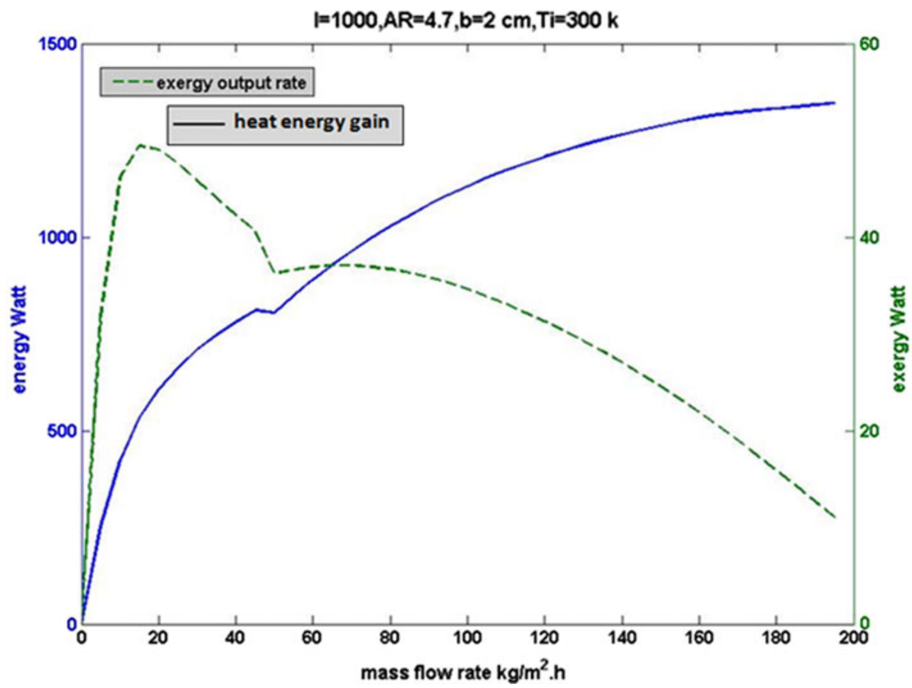

Fig. 4 Variation of exergy output rate and heat gain rate with mass flow rate with low inlet temperature of air

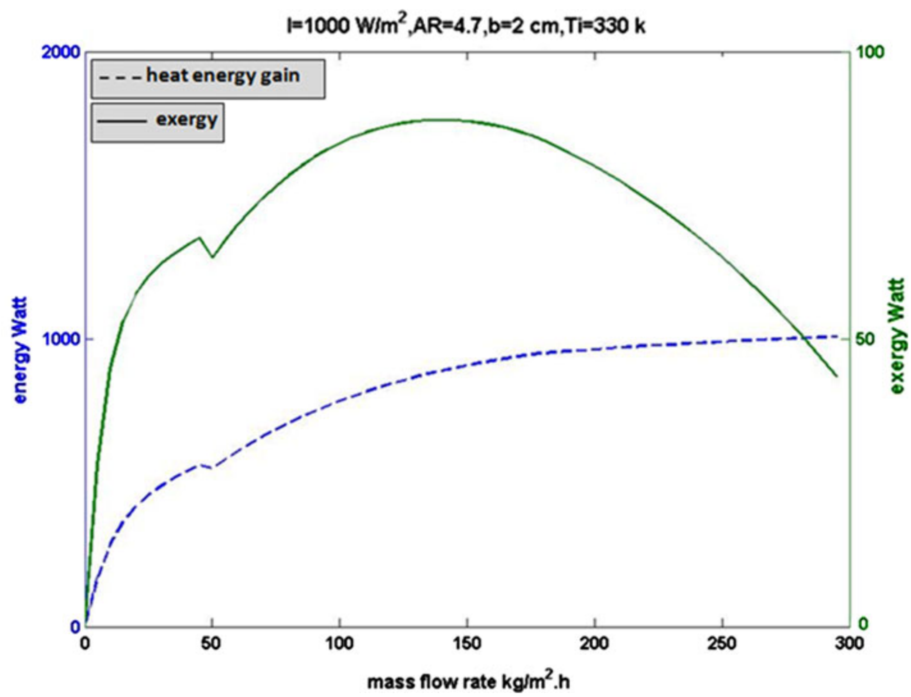

Fig. 5 Variation of exergy output rate and heat gain rate with mass flow rate with high inlet temperature of air

to reach a peak and then descends to become negative in higher rates of mass flow. As the inlet air temperature increases from $T_i =$ 300 to 330 K, the exergy peak shifts from 49.43 to 88.07 W. So for getting higher rate of exergy output in case of low inlet temperature of air it is more rational to keep the mass flow rate lower in comparison with the case of higher temperature of inlet air.

Hence, the interaction of both inlet air temperature and mass flow rate on exergy should be studied simultaneously to find the true range of mass flow rate for getting a higher rate of exergy. To gain such a goal, variations of energy and exergy with temperature and mass flow rates are shown in the 3 dimensional diagram brought in Figs. 6 and 7.

It is clearly observed that energy output rate generally follows an increasing trend with mass flow rate and it may be attributed to higher heat removal capability of flowing air from the absorber and consequently lower heat losses, while the exergy output rate after experiencing an increasing trend will follow a descending trend.

But higher inlet temperatures of air with a fixed mass flow rate lead to increase of exergy and decrease of energy. This phenomenon may be rational as increasing inlet air temperature brings about the increase of heat losses and useful energy gain is decreased while the decrease rate of entropy created is higher than loss of heat gain and the difference representing exergy experiences an increasing trend.

4.3 Variations of heat energy gain and exergy output rate with mass flow rate and triangular duct altitude

Figures 8 and 9 show the variations of energy and exergy output rates with mass flow rate and different values of triangular duct altitude (b), respectively. Based on AR definition as the ratio of length to width of the collector, for a fixed collector area and the apex angle of each triangle 60°, there exists a relation between b and width of collector and AR as the result as one can replace the other parameter. The inlet temperature is considered equal to ambient temperature. It is clear from Fig. 8 that the energy output rate is higher at lower values of duct altitudes, so for higher energetic performance of the collector the altitude should be lower. The exergy output rate does not follow the same trend as that of energy and does not have a monotonous trend (Fig. 9) with mass flow rate. At low mass flow rates the exergy rate is also high for lesser duct altitudes while it decreases faster with mass flow rate. There for, for achieving higher rate of exergy, the lower b is recommended when the rate of mass flow is also low.

4.4 Variations of energy and exergy efficiencies with mass flow rate

Figure 10 shows the variations of energy and exergy efficiencies with mass flow rate while the inlet air temperature is assumed equal to the ambient air temperature. As seen, energy efficiency has a monotonously increasing trend with mass flow rate while exergy efficiency follows a descending trend after a sharp increase through the laminar flow of the fluid. Exergy efficiency with fixed values of radiation intensity, AR and inlet air temperature becomes negative after a specified mass flow rate.

For better understanding, in Fig. 11 the simultaneous effects of mass flow rate and inlet air temperature on exergy efficiency are demonstrated. As clearly shown,

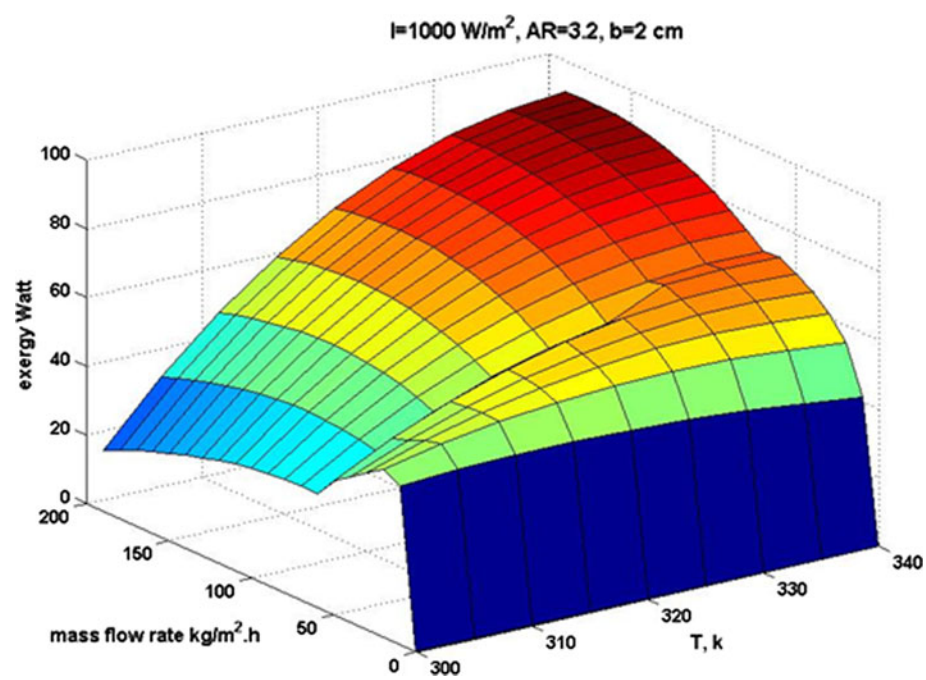

Fig. 6 Variation of exergy output rate with mass flow rate and inlet temperature of air for a solar radiation intensity of 1,000 W/m^2

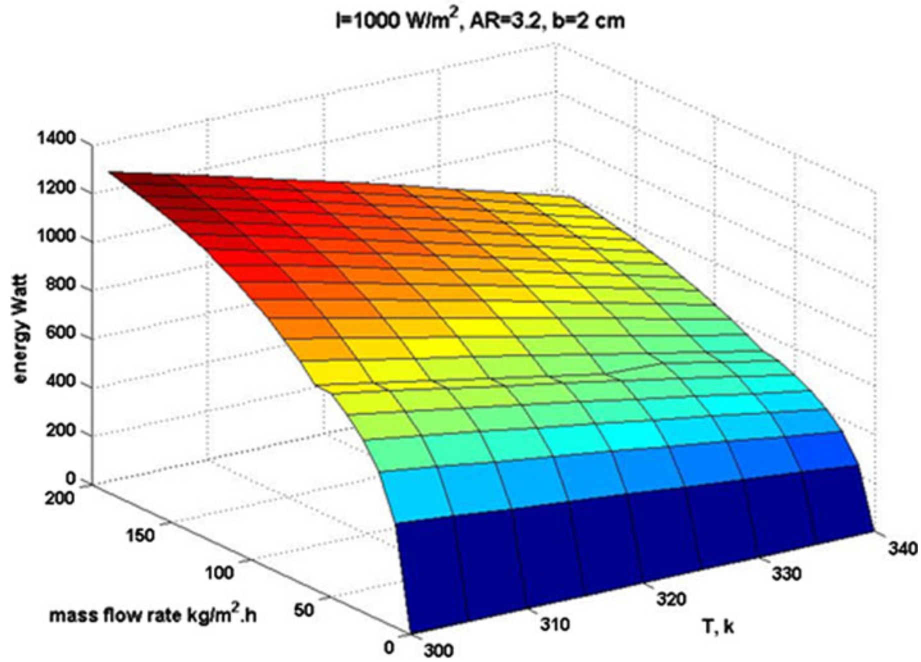

Fig. 7 Variation of heat gain rate with mass flow rate and inlet temperature of air for a solar radiation intensity of 1,000 W/m^2

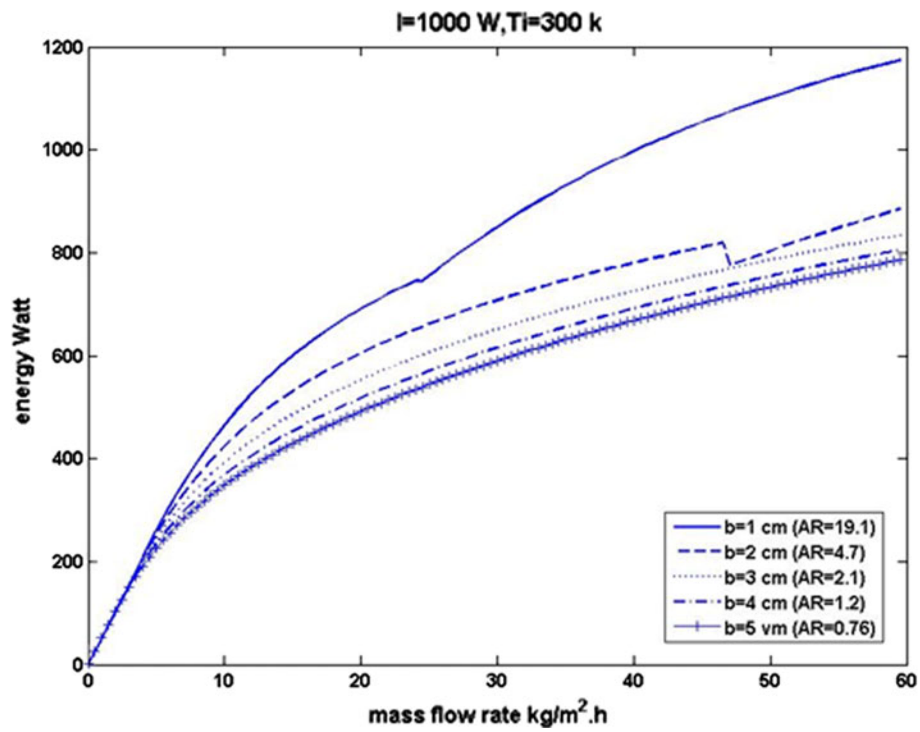

Fig. 8 Variation of energy heat gain with mass flow rate and triangular duct altitude

exergy efficiency increases with mass flow rate, on condition that it accompanies with higher temperature of inlet air which is consistent with the results obtained in the previous sections. During the day that SAH are mostly used for heating and drying purposes, from morning to noon naturally the inlet air temperature increases and it lets us to increase the mass flow rate of flowing air through the duct for gaining higher rate of energy and exergy efficiencies. But it requires a kind of a sensor which can monitor the inlet air temperature at time intervals and through an electronic control circuit can adjust the pump speed based on that temperature.

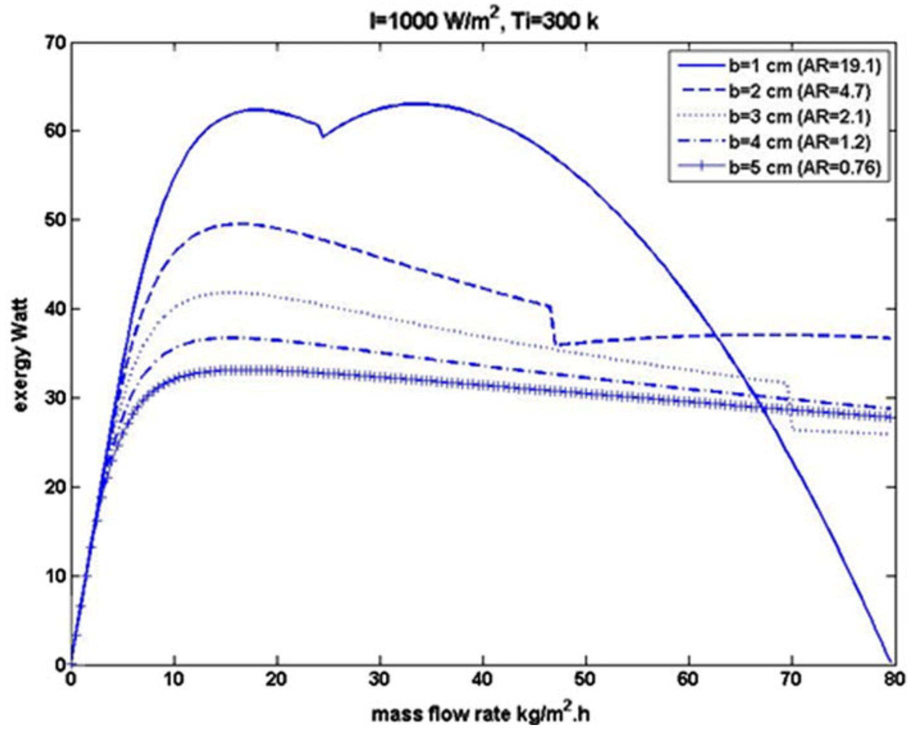

Fig. 9 Variation of exergy output rate with mass flow rate and triangular duct altitude

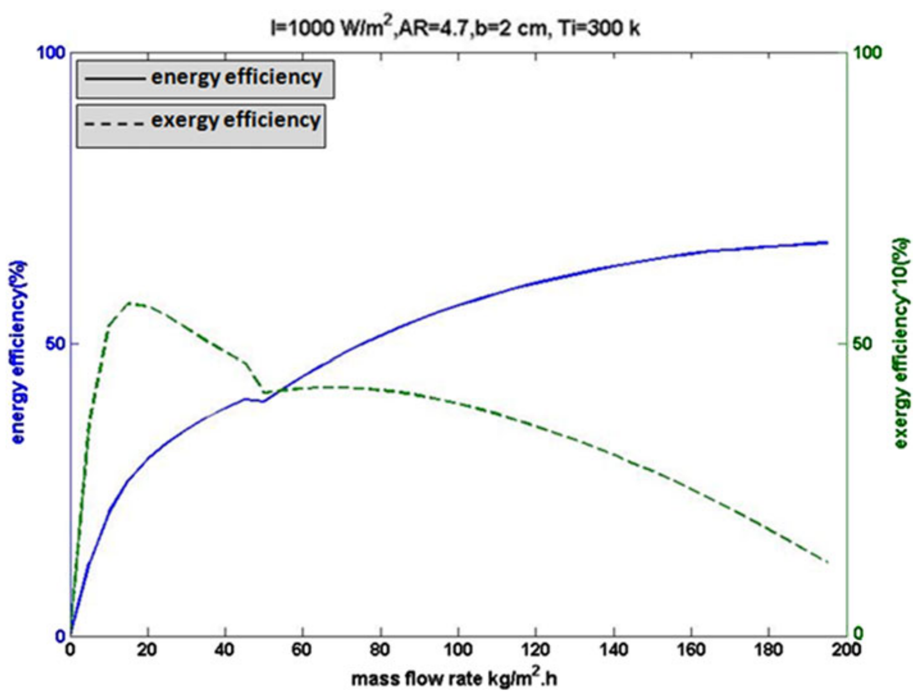

Fig. 10 Variation of energy and exergy efficiencies with mass flow rate for radiation intensity of 1,000 W/m^2 and inlet temperature of 300 K

4.5 Variations of exergy with mass flow rate and number of glass covers

Figure 12 shows the variation of exergy output rate with mass flow rate and number of glass covers. Increasing the number of glass covers brings about higher values of exergy. It is evident that the effect of number of glass covers on exergy is more significant through the laminar regime and as it shifts to turbulent one such effect is lesser obvious. From the other aspect, a very important factor for

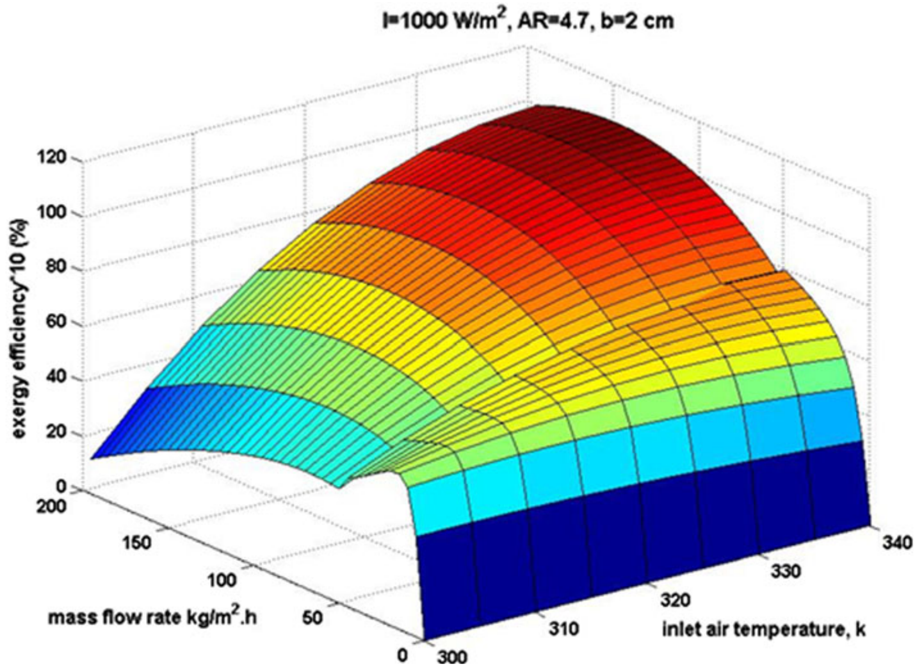

Fig. 11 Variation of exergy efficiency with mass flow rate and inlet air temperature

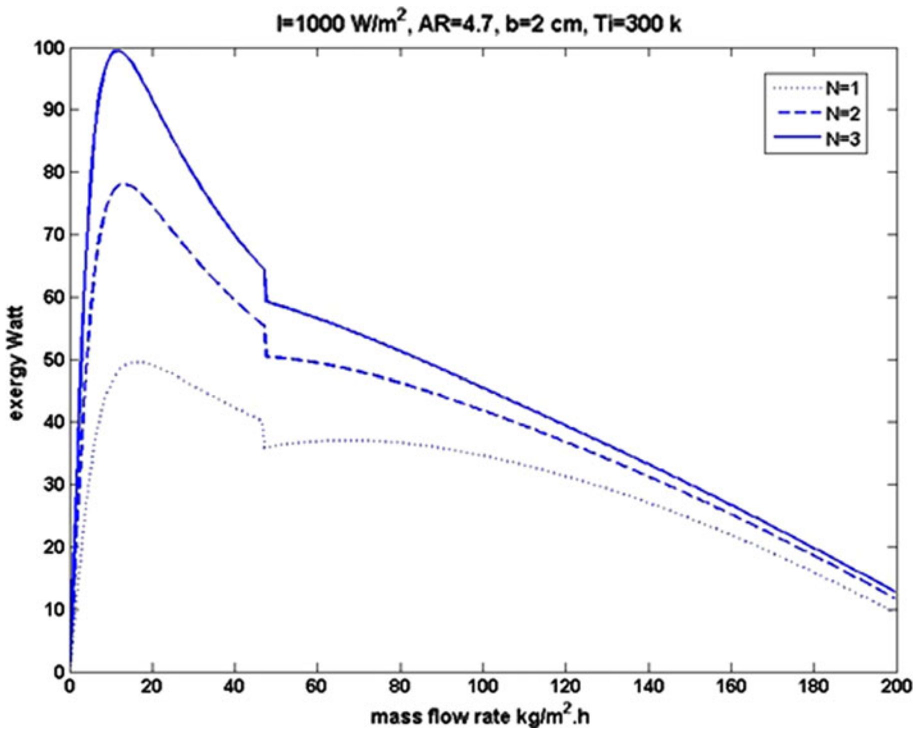

Fig. 12 Variation of exergy with mass flow rate for different number of glass covers

deciding about the collector specifications is the economic perspective. As glass cover is a major collector component which its price has a significant impact on the whole costs of the collector, hence it must be investigated whether the increase in exergy due to more number of covers has priority to this cost increase or not i.e. a tradeoff between these two effective parameters should be investigated.

5 Conclusions

In this paper, the parametric and exergetic study of a v-corrugated solar air heater is conducted. It can be said that as per the energy output rate evaluation criterion to reach higher rate of energy from the v-corrugated solar air heater it is highly recommended to have high AR, and low altitude of triangular duct and mass flow rate and try to keep the temperature of the inlet air as low as possible. The exergy output for a specified rate of mass flow is dependent on the difference between the values of energy and entropy created term; it is clearly observed that if the inlet temperature of air is low then the maximum exergy output is achieved with low values of mass flow rates rate but if the inlet temperature of air is high then exergy output increases with mass flow rate to reach a peak and follows a descending trend if we exceed such a limit. The effect of AR on energy and exergy outputs shows that high AR leads to higher rate of energy and exergy generally; from the other point of view, low possible triangular ducts bring about decrease in energy and exergy outputs. Finally, more number of glass covers leads to better exergy outputs while the decision about the number of it should consider the economical aspect of it.

Acknowledgments The authors are highly grateful to the University of Tabriz for giving all types of support.

References

1. Alvarez G, Arce J, Lira L, Heras MR (2004) Thermal performance of an air solar collector with an absorber plate made of recyclable aluminum cans. Sol Energy 77:107–113
2. Karim MA, Hawlader MNA (2006) Performance investigation of flat plate, v-corrugated and finned air collectors. Energy 31:452–470
3. Esen H (2008) Experimental energy and exergy analysis of a double-flow solar air heater having different obstacles on absorber plates. Build Environ 43:1046–1054
4. Akpinar EK, Koçyiğit F (2010) Energy and exergy analysis of a new flat-plate solar air heater having different obstacles on absorber plates. Appl Energy 87:3438–3450
5. Alta D, Bilgili E, Ertekin C, Yaldiz O (2010) Experimental investigation of three different solar air heaters: energy and exergy analyses. Appl Energy 87:2953–2973
6. Tyagi VV, Pandey AK, Giridhar G, Bandyopadhyay B, Park SR, Tyagi SK (2011) Comparative study based on exergy analysis of solar air heater collector using thermal energy storage. Int J Energy Res. doi:10.1002/er.1827
7. Tyagi SK, Shengwei W, Singhal MK, Kaushik SC, Park PR (2007) Exergy analysis and parametric study of concentrating type solar collectors. Int J Therm Sci 46:1304–1310
8. Farahat S, Sarhaddi F, Ajam H (2009) Exergetic optimization of flat plate solar collectors. Renew Energy 34:1169–1174
9. Bejan A (1988) Advanced engineering thermodynamics. Wiley Interscience, New York, p 133
10. Öztürk HH, Demirel Y (2004) Exergy-based performance analysis of packed-bed solar air heaters. Int J Energy Res 28:423–432
11. Öztürk HH (2005) Experimental evaluation of energy and exergy efficiency of a seasonal latent heat storage system for greenhouse heating. Energy Convers Manag 46:1523–1542
12. Ucar A, Inalli M (2006) Thermal and exergy analysis of solar air collectors with passive augmentation techniques. Int Commun Heat Mass 33:1281–1290
13. Kurtbas I, Durmus A (2004) Efficiency and exergy analysis of a new solar air heater. Renew Energy 29:1489–1501
14. Gupta MK, Kaushik SC (2009) Performance evaluation of solar air heater for various artificial roughness geometries based on energy, effective and exergy efficiencies. Renew Energy 34:465–476
15. Hepbasli A (2008) A key review on exegetic analysis and assessment of renewable energy sources. Renew Sust Energy Rev 12:593–661
16. Suzuki A (1988) General theory of exergy-balance analysis and application to solar collectors. Energy 13:153–160
17. Lin W, Gao W, Liu T (2006) A parametric study on the thermal performance of cross-corrugated solar air collectors. Appl Therm Eng 26:1043–1053
18. Qi Z, Chen J, Chen Z (2007) Parametric study on the performance of a heat exchanger with corrugated louvered fins. Appl Therm Eng 27:539–544
19. Verma R, Chandra R, Garg HP (1991) Parametric studies on the corrugated solar air heaters with and without cover. Renew Energy 1:361–371
20. Parker BF, Lindley MR, Colliver DG, Murphy WE (1993) Thermal performance of three solar air heaters. Sol Energy 51:467–479
21. Liu T, Lin W, Gao W, Luo C, Li M, Zheng Q, Xia C (2007) A parametric study on the thermal performance of a solar air collector with a v-groove collector. Int J Green Energy 4:601–622
22. Duffie JA, Beckman WA (1991) Solar engineering of thermal processes, 2nd edn. Wiley, New York
23. McAdams WH (1954) Heat transmission, 3rd edn. McGraw-Hill, New York
24. Hollands KGT, Shewen EC (1981) Optimization of flow passage air-heating, plate-type solar collector. J Sol Energy Eng 103:323–330
25. Gao W, Lin W, Liu T, Xia C (2007) Analytical and experimental studies on the thermal performance of cross-corrugated and flat-plate solar air heaters. Appl Energy 84:425–441
26. Gupta MK, Kaushik SC (2008) Exergetic performance evaluation and parametric studies of solar air heater. Energy 33:1691–1702
27. Hegazy AA (2000) Thermohydraulic performance of air heating solar collectors with variable width, flat absorber plates. Energy Convers Manag 41:1361–1378